Petroleum and Coal

Article Open Access

Subsurface Characterization Using Seismic Refraction Tomography in the University of Port Harcourt

Rasaq Bello[1], Jonathan ChineduNwafor[2]

[1] Department of Physics, Federal University Kashere, Gombe State, Nigeria
[2] Department of Physics, University of Port Harcourt, Port Harcourt, Nigeria

Received July 5, 2018; Accepted September 28, 2018

Abstract

Seismic refraction tomography survey was carried out in four different sites (profiles) for the subsurface characterization. Results showed that the study areas are made-up of three layers and there is an increase in velocity with depth in the areas. The first layer is the weathered layer and is suggested to be dry sand. It has average thicknesses of 12.49 m, 9.17 m, 11.71 m, and 11.73 m, and velocity ranges from 779 m/s to 1531 m/s, 822 m/s to 1487 m/s, 846 m/s to 1480 m/s and 837 m/s to 1475 m/s respectively for the four profiles. The second layer is thought to be saturated sand (aquifer layer) and has average thicknesses of 2.9 m, 2.8 m, 2.0 m and 2.3 m at depths of 12.49 m, 9.17 m, 11.71 m and 11.73 m with velocities ranges from 1531 m/s to 2068 m/s, 1487 m/s to 2073 m/s, 1480 m/s to 2026 m/s and 1475 m/s to 2006 m/s respectively along the profiles. The third layer which is thought to be sand stone at depths 15.39 m, 11.97 m, 13.66 m and 13.99 m, and has infinite thicknesses with velocities ranges from 2068 m/s to 4216 m/s, 2073 m/s to 4157 m/s, 2026 m/s to 4621 m/s and 2006 m/s to 4237 m/s respectively along the profiles.

Keywords: *Seismic; Refraction; Tomography; Lithology; Profiles.*

1. Introduction

The first geophysical approach used in search of the reservoir is the seismic refraction method, but over the years its relevance in the exploration of oil has reduced because of different types of modern reflection studies. Though, seismic refraction survey is continually relevance on the shallow investigation of the subsurface, especially for civil and geotechnical engineering sites. It remains non negligible exploratory instrument for a shallow survey when applied together with investigative drill [1]. The two ways travel time is measured in a refraction survey at a known place on the Earth along its surface where the seismic primary (P) waves energy is generated via an energy source. The energy source is usually generated through a small explosive charge, vibrosis or accelerated weight drop [2]. The energy which radiates from the shot point traveled via the top layer and refracted on a boundary, and then detected at the surface by geophones (12, 24, 48, or more geophones) that are arranged in linear array whereas travel times are recorded via seismometer. Graphs of geophone distance (starting from the first geophone to the last) against time of those first arrivals are plotted to show the depth to refracting interfaces. "Seismic refraction method is quantitative as it produces depths of various geo-material layers and the compressional wave velocity *(*V_p*)* of these layers" [3].

Seismic refraction tomography is a method for examining the Earth's interior with seismic wave generated by earthquakes or explosions. P-, S-, and surface waves can be used for tomographic models of different resolutions based on seismic wavelength, the seismograph array coverage, and wave source distance. The seismic refraction tomography (velocity gradient or diving-wave tomography) employs first arrival travel time of seismic wave for its input. In this method, both forward and reverse shots are taken by firing shots before the first geophone and after the last geophone respectively, and shots are also fired at various points of geophones which make it possible to scan every point of the Earth's interior of the profile line from both forward and reverse shot. Although the depth of probe depends mainly on the energy source (explosive, vibrosis or weight drop) and geophones spacing along the profile, that means the higher the geophone spacing is higher the depth of probe. The spatial variations such as pore fluids, fracturing, or lithology, maybe forecasted from the information obtained from seismic refraction tomography technique. Hence, the technique is of great importance in applications to engineering and greater extent of exploration [4]. Seismic refraction tomography survey was carried out in four different sites in the University of Port Harcourt with a total length of 95 mands 5 m being geophone spacing.

1.1. Geology of the study area

The study area of the first site (behind faculty of Social Sciences) has coordinates of latitude 04°54'28.5" North and longitude of 006°55'06.8" East with an elevation of 17.2 m, the second site (front of faculty of humanity) has coordinates of latitude 04°54'29.1" North and longitude of 006°55'09.3" East with an elevation of 17.4 m, the third site (behind Gas Engineering Department) has coordinates of latitude 04°54'26.0" North and longitude of 006°55'25.4" East with an elevation of 17.0 m, while the fourth site (adjacent to Gas Engineering Department) has coordinates of latitude 04°54'25.1" North and longitude of 006°55'23.0" East with an elevation of 17.1 m, all in the University of Port Harcourt, Obio/Akpor Local Government Area of Port Harcourt Metropolis, Rivers State of Nigeria.

1.2. Stratigraphic framework

The sequential order of the Niger Delta layers is made up three wide lithostratigraphic units and they are, (1) Benin Formation (sequence of a continental shallow massive sand), (2) Agbada Formation (a costal marine sequence of alternating sands and shales) and (3) Akata Formation (a basal marine shale unit) [5-8]. Clays and Shales including minor sand intercalations are the components of the Akata Formation. They were deposited prodelta environments and sand deposited here is less than 30% in general.

Sands and shales are the components of Agbada Formation signifying sediments of the transitional environment consist of the lower delta plain (mangrove swamps, marsh, flood plain) and the coastal barrier and fluviomarine realms. In the Agbada Formation sand varies in percentage from 30-70%, which is as a result of more large numbers of depositional offlap cycles. Generally, a complete cycle is made-up of minor fossiliferrous transgressive marine sand, followed by an offlap sequence which commences with marine shale and continues with laminated fluviomarine sediments followed by barriers and/or fluviatile sediments terminated by another transgression [5].

The Benin Formation is made-up of high sand which varies in percentage from 70-100% and forms the outermost Niger Delta layers depositional sequence. The huge sands were placed in a continental setting comprising the fluvial realms (braidedand meandering systems) of the top delta plain.

2. Methodology

2.1. Data acquisition

All the data used in this research were acquired using seismic refraction tomography survey with instruments Seismometer; Twelve geophones, Cable, Weight drop (sledge hammer), Base plate, GPS (Global positioning system), Cutlass, Umbrella, Trigger geophone, Trigger cable realm, Tape and Wooden pegs, in the University of Port Harcourt, Abuja campus. The data were gotten in four different places, behind the Faculty of Social Sciences (first profile), in the front of the Faculty of Humanities (second profile), behind Faculty of Gas Engineering (third profile), and adjacent to the Faculty of Gas Engineering (fourth profile). The data were acquired in a relatively calm environment, and efforts were put in place to assure that random noise was suppressed as much as possible. Though all the obtainable sources of the random noise could not be stopped because of the nature of the environment (school activities), but yet it was controlled to a reasonable extent. The profiles where the data were obtained have approximately zero gradients and structures were erected on the surroundings. The first and second profiles were about 120 m and 170 m respectively away from the road while the third and fourth profiles were 200 m and 100 m respectively away from the road.

Shot points and geophone positions were first marked starting from one end marking 5 m and using wooden pegs to separate them to the other end. A total of twenty points were made for both forward and reverse shots. Twelve geophones were then fixed as shown in figure 1 connecting to the cable with their polarity being observed. The cable and trigger cable realm connecting to trigger geophone positioned in a shot point were connected properly to ABEM seismometre being powered by a DC battery. Vertical geophones were properly placed perpendicular to the Earth's surface in order to pick the vibration made by the ground.

A total length of 95 m was used for each profile line (shown in Figure.1). Sledge hammer was, used as the energy source. In order to reduce the random noise, five stacks were made, and the averathe ges were recorded by the seismometer on each shot point.

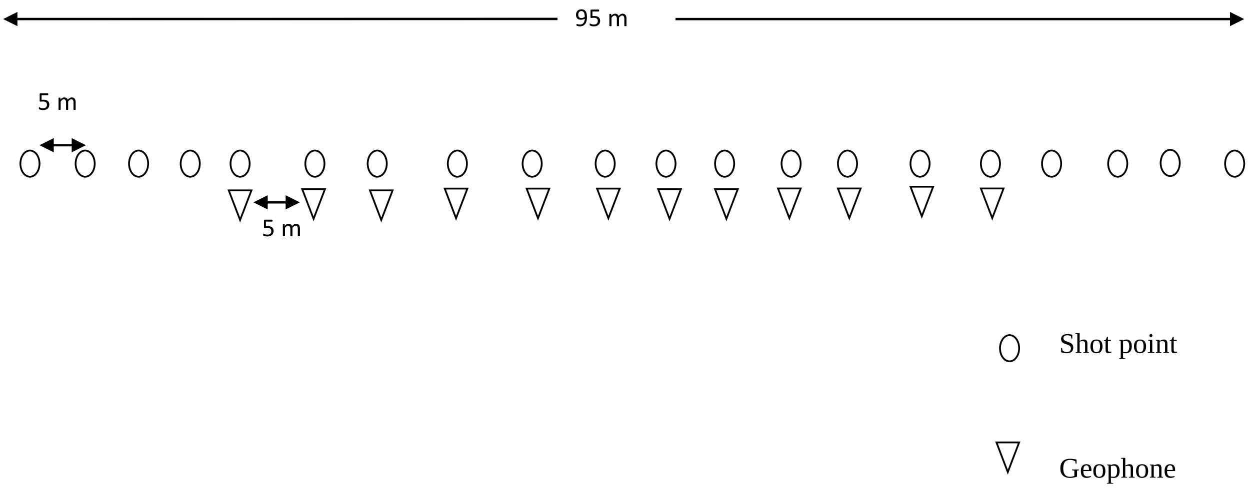

Figure 1. The profile line showing geophone and shot points positions in the site

2.2. Data processing

After the data had been acquired from the field using the adequate instruments listed above, the next step was the extraction of data from the seismometer for processing. The data was extracted by connecting the seismometer into a computer system providing access to the raw data. The raw data which has no value until it was processed by appropriate software like Reflexw is of SEG2 file type. The first step in processing was to import the data in the Reflex as a SEG2 format. The data were imported into the software as a SEG2 format to enable the software to recognize them as seismic data. At this stage, the outline used in the site was provided to the software for proper processing, for example, number of shot points and geophone spacing, number of geophones used and others. After the importation of data, the next stage is to filter out the noise and then gaining.

After importing the data which always comes with random noise, the next stage is to filter out the noise. Both random noise (noise coming from the environment such as vibration caused by car) and coherent noise (noise coming from the instrument maybe due to malfunction) in the data obscure the subsurface imaging, therefore, have to filter out in order to observe a comprehensible image about the subsurface. By filtering, bandpass frequencies of 20 Hz for lower cutoff and 50 Hz for upper cutoff were applied. Gaining (Deconvolution) is applied immediately the data is filtered. By gaining, amplification of the amplitude of the signal which was reduced as it propagates through the Earth and spread its energy over a large surface was achieved.

After enhancing the amplitude of the signal which gives room to identify the first refractor, the next is to careful pick the time it takes each geophone to record signal picked from the first interface by a particular source signal generation known as first arrival travel times or first breaks. This was carried out by manual picking.

From the picking of the first arrival travel times for each shot, time-distance graph for forward and reverse shots were plotted (see Fig. 2). Travel times are recorded in milliseconds for both forward and reverse shots. The average refracted travel time is calculated which we used to assign layers.

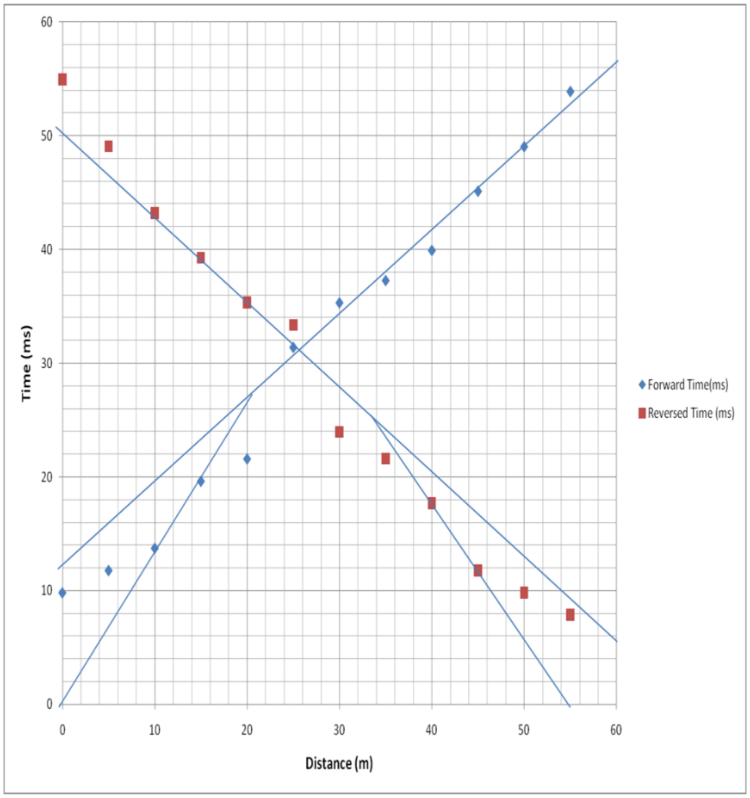

Figure 2. Time-distance graph for first shot arrival travel times picked for both forward and reversed shots of the 1st profile line

The next is the wavefront inversion. By inversion, velocity-depth models directly from the recorded data are produced (see Fig. 3-6). The picked traveltimes of different shots are put together by traveltime processing (the first part) which also assign picks to special layers. The wavefront inversion method is used to invert the combined traveltimes into the underground model and hence allows: interactive back propagation of the wavefronts using finite differences approximation of the eikonal equation; the back propagation is exact, even for very complicated overburdens [9].

After the models were generated by wave front inversion, ray tracing was then applied. In a system which has regions of varying propagating velocity, absorption characteristics, and reflecting surfaces, ray tracing is seen as a technique used to calculate the path of particles or waves. Under these conditions, wave fronts may change direction, bend, or reflect off surfaces, complicating analysis. Ray tracing correct the setback by constantly advancing idealized thin beams called rays through the system by discrete amounts [10]. From this analysis, the tomography models were generated for the four profiles in the study areas.

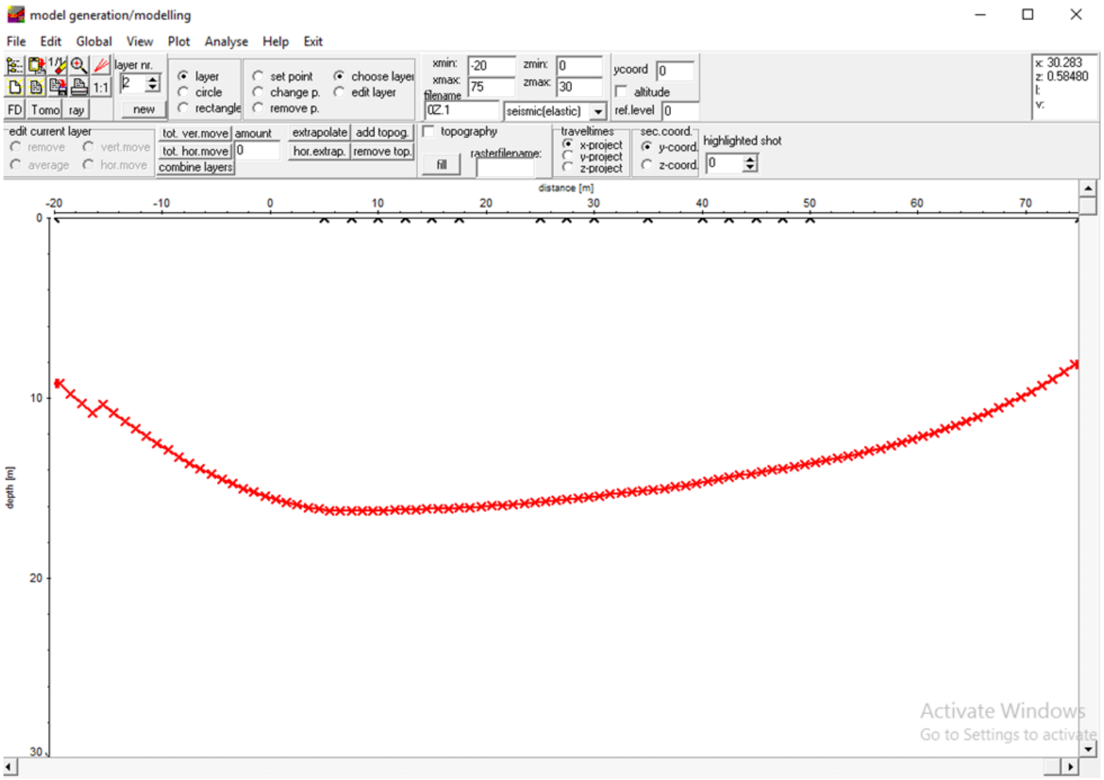

Figure 3. The first profile inversion process with Reflex software to generate initial first and second layers. The model showing initial depth of the weathered layer in lateral direction of the profile

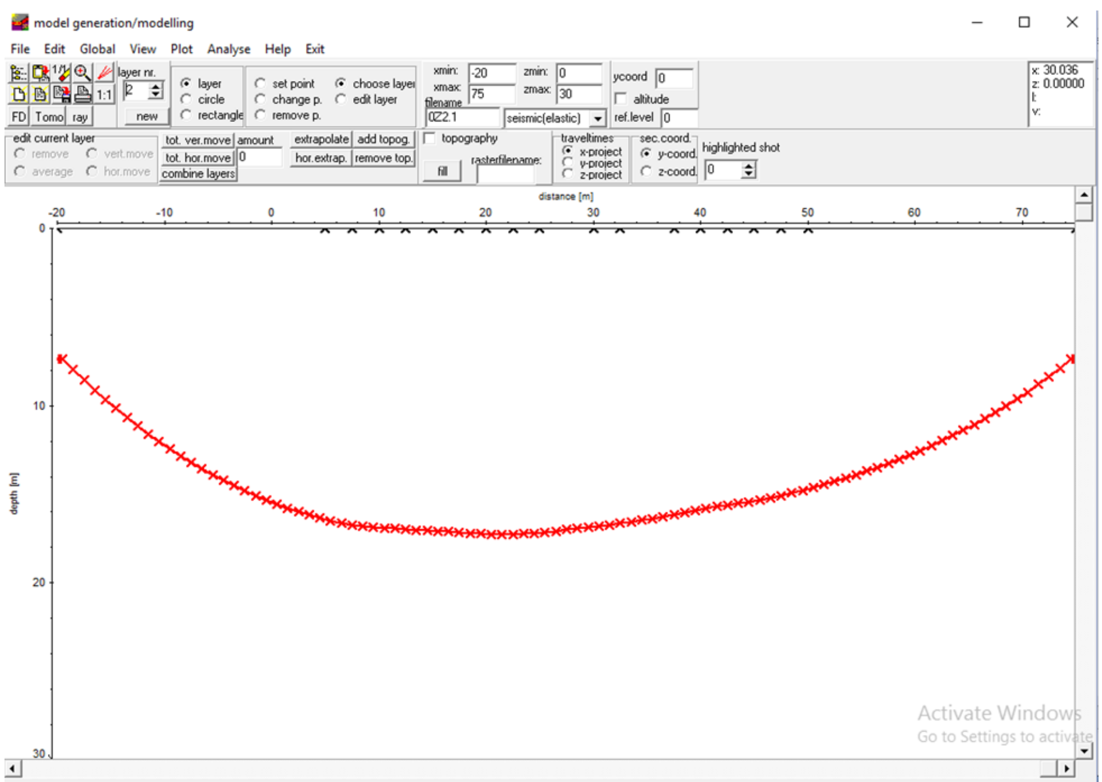

Figure 4. Second profile inversion process with Reflex software to generate initial first and second layers. The model showing initial depth of the weathered layer in lateral direction of the profile

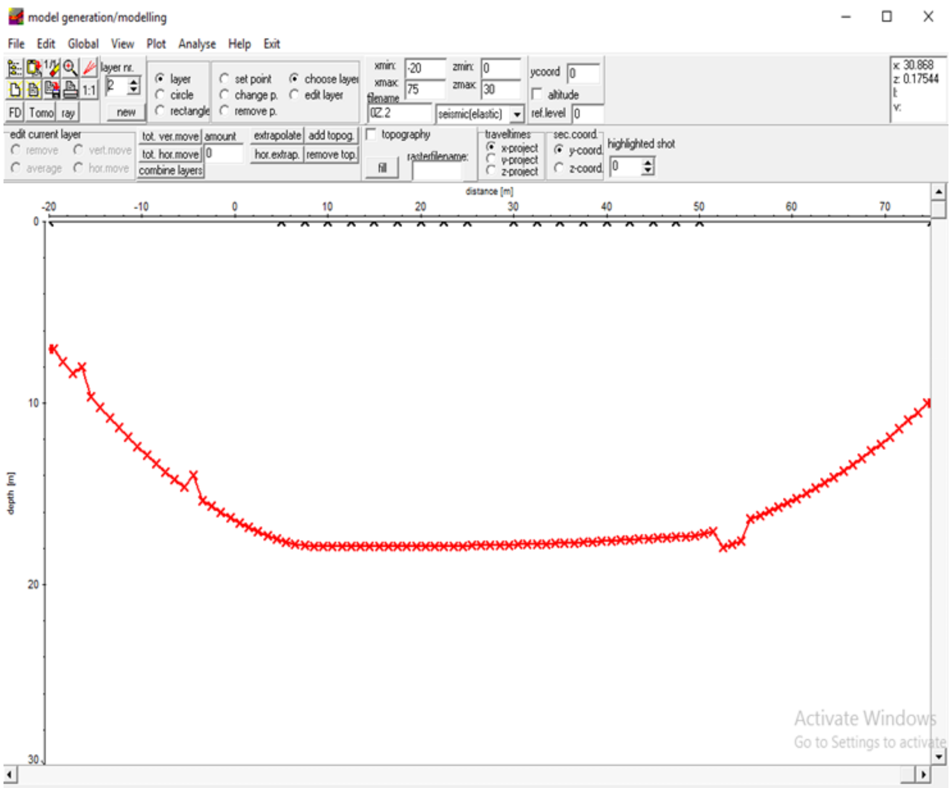

Figure 5. Third profile inversion process with Reflex software to generate initial first and second layers. The model showing initial depth of the weathered layer in lateral direction of the profile

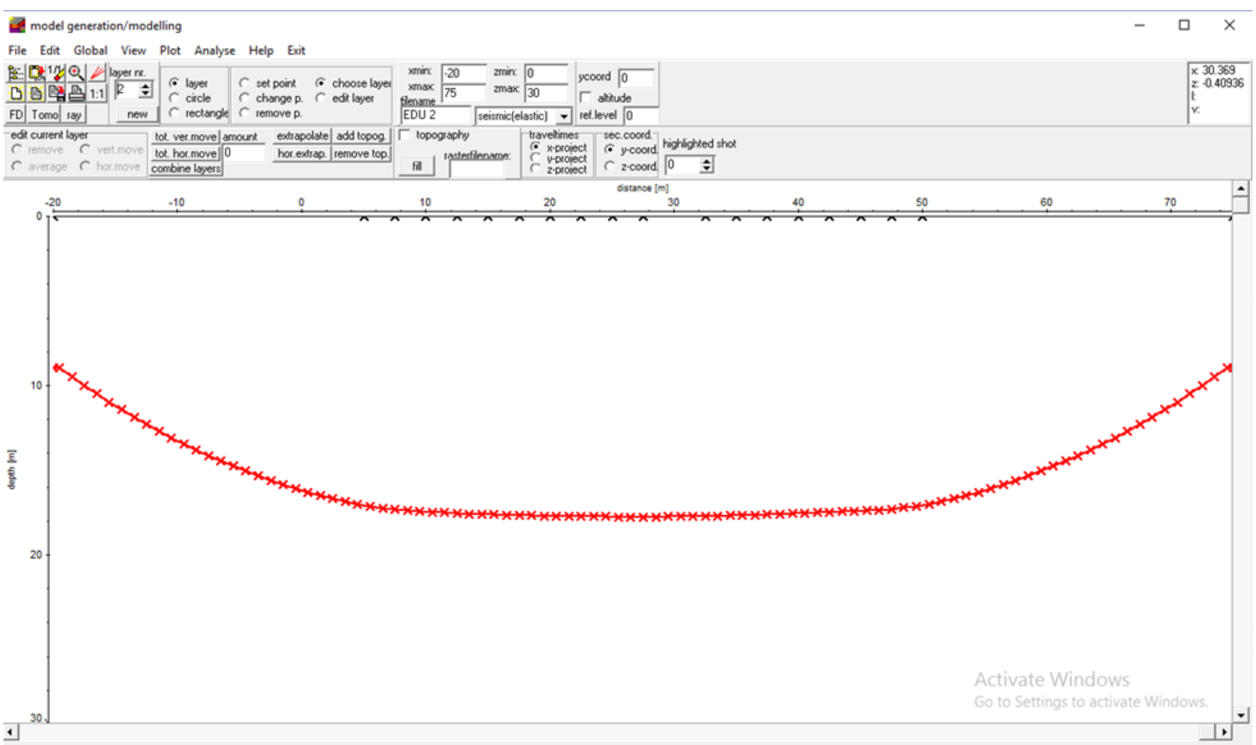

Figure 6. Fourth profile inversion process with Reflex software to generate initial first and second layers. The model showing initial depth of the weathered layer in lateral direction of the profile

Table 1. First shot arrival travel times picked for both forward and reversed shots of the 1st profile line

Distance (m)	Forward Time (ms)	Reversed Time (ms)
0	9.81	54.93
5	11.77	49.04
10	13.73	43.16
15	19.62	39.23
20	21.58	35.31
25	31.39	33.35
30	35.31	23.95
35	37.27	21.58
40	39.92	17.66
45	45.12	11.77
50	49.04	9.81
55	53.89	7.85

3. Results and discussion

The velocity tomography models for first to fourth profiles are respectively shown in Figure 7 to Figure 10. The velocity tomography models are presented in different shades of colours. The velocity distributions portrayed by the tomography models show an increase in velocity with depth along the whole profiles. There is no case or evidence where a low velocity layer is overlain with higher velocity layer. By the right hand side of each tomography model, a colour bar is attached to it showing velocity range of each colour. The tomography models are not discussed based on the colour distributions in the models but are discussed according to the velocity distribution attached to a colour from the colour bar. From the tomography models, a horizontal distance along the profile is shown in meters also, a vertical distance showing the depth of probe measured in meters. The tomography models clearly isolated the consolidated from the unconsolidated layer (weathered layer).

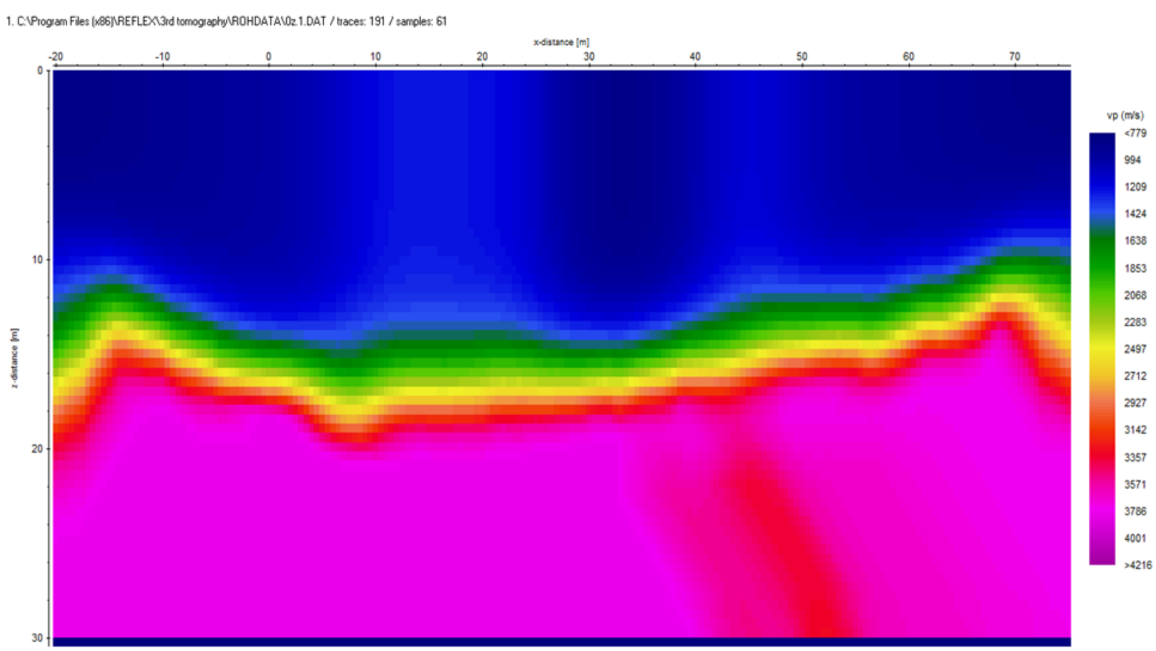

Figure 7. Tomography model of velocity distribution along the first profile

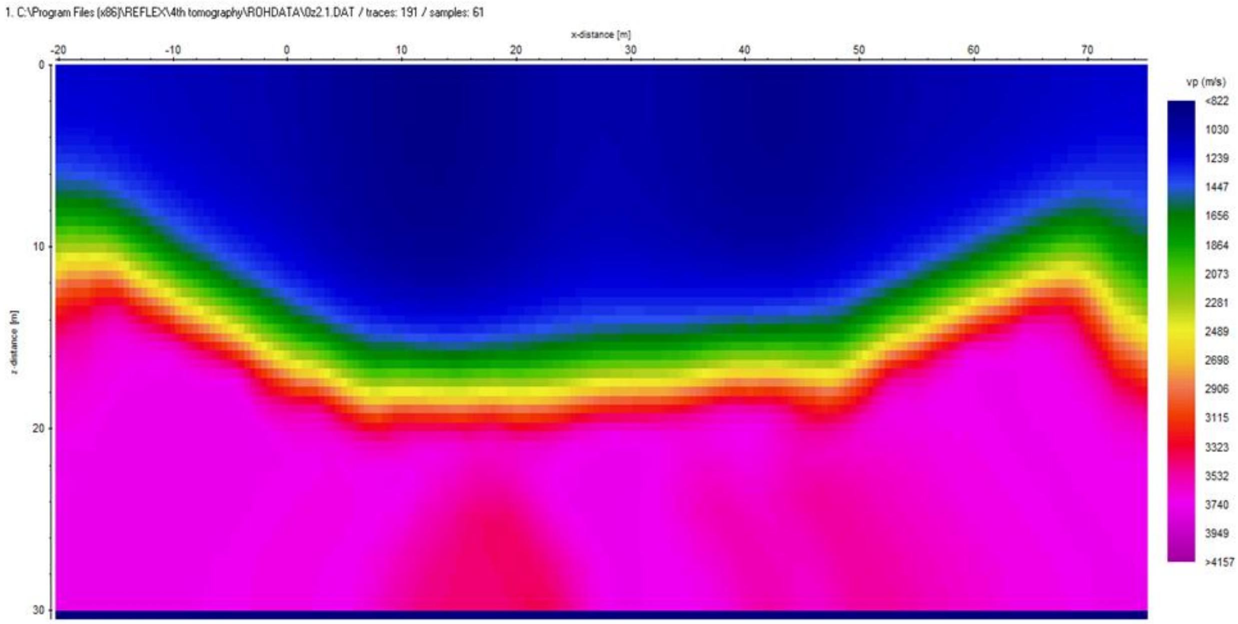

Figure 8. Tomography model of velocity distribution along the second profile

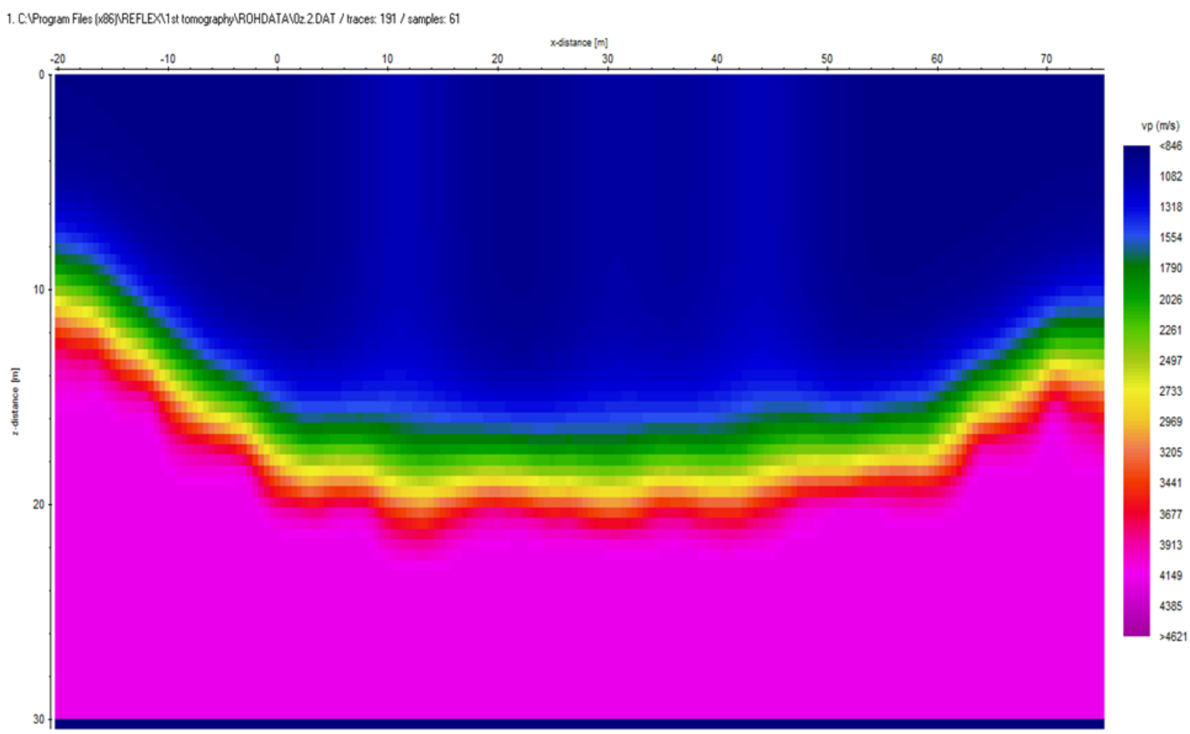

Figure 9. Tomography model of velocity distribution along the third profile

For the first profile, the surface velocity down to the entire depth of the probe from the tomography model as shown in Figure 2 ranges from 779 m/s to 4216 m/s. The model shows the weathered layer primary wave velocity varies from 779 m/s to 1531 m/s. The weathered layer thickness is 11.59 m at the beginning, 14.33 m at the middle, and 9.22 m at the end with an average thickness of 12.49 m. The following layer has p-wave velocity varies from

1531 m/s to 2068 m/s at an average depth of 12.49 m. While the velocity of the third layer varies from 2068 m/s to 4216 m/s at an average depth of 15.39 m along the profile.

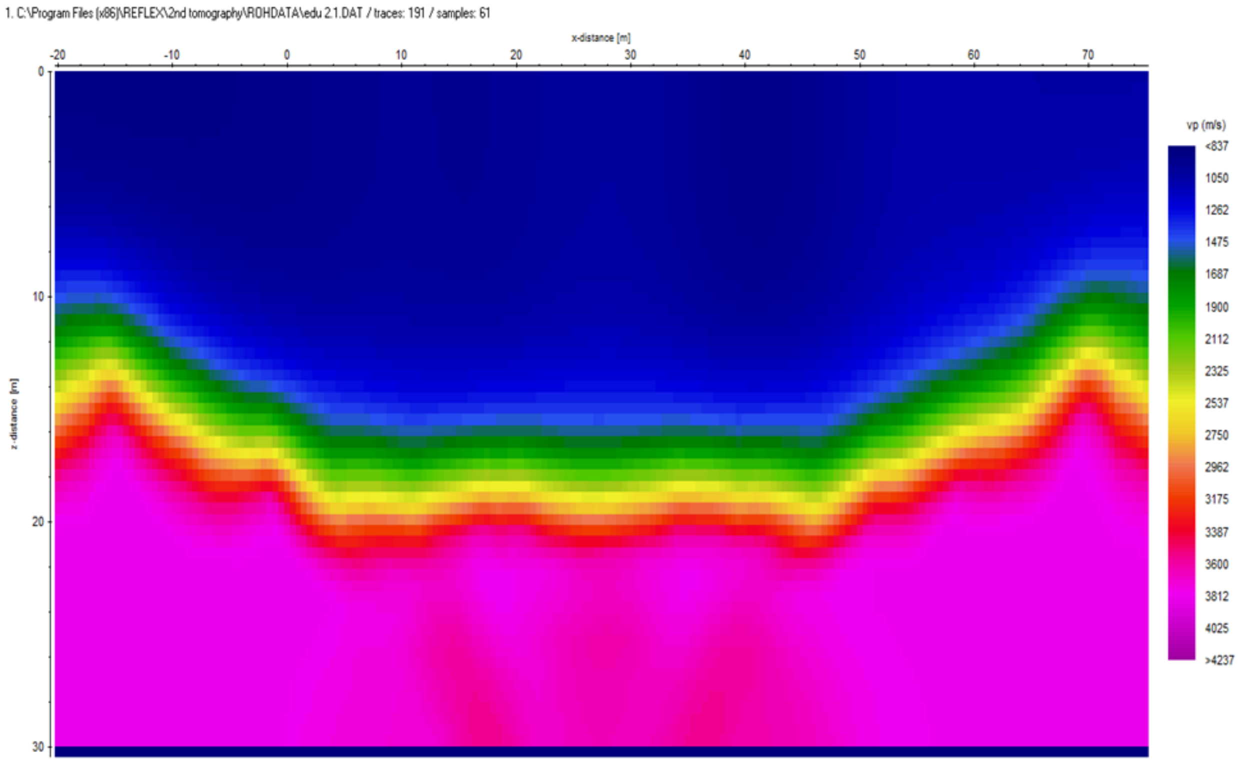

Figure 10. Tomography model of velocity distribution along the fourth Profile

The surface velocity down to the entire depth of the probe from the tomography model of the second profile as shown in Figure 3 ranges from 822 m/s to 4157 m/s. The weathered layer primary wave velocity varies from 822 m/s to 1487 m/s. The weathered layer thickness is 6.27 m at the beginning, 14.01 m at the middle, and 7.22 m at the end with an average thickness of 9.17 m. The following layer has p-wave velocity varies from 1487 m/s to 2073 m/s at an average depth of 9.17 m. While the velocity of the third layer varies from 2073 m/s to 4157 m/s at an average depth of 11.97 m along the profile.

Also, the surface velocity down to the entire depth of the probe from the tomography model of the third profile showed in Figure 4.4 ranges from 846 m/s to 4621 m/s. The weathered layer primary wave velocity varies from 846 m/s to 1480 m/s. The weathered layer thickness is 8.01 m at the beginning, 16.38 m at the middle, and 10.75 m at the end with an average thickness of 11.71 m. The following layer has p-wave velocity varies from 1480 m/s to 2026 m/s at an average depth of 11.71 m. While the velocity of the third layer varies from 2026 m/s to 4621 m/s at an average depth of 13.66 m along the profile.

Then, the surface velocity down to the entire depth of the probe from the tomography model of the fourth profile showed in figure 5 ranges from 837 m/s to 4237 m/s. The weathered layer primary wave velocity varies from 837 m/s to 1475 m/s. The weathered layer thickness is 10.17 m at the beginning, 16.01 m at the middle, and 8.96 m at the end with an average thickness of 11.73 m. The following layer has p-wave velocity varies from 1475 m/s to 2006 m/s at an average depth of 11.73 m. While the velocity of the third layer varies from 2006 m/s to 4237 m/s at an average depth of 13.99 m along the profile.

The four tomographic models have three equivalent layers and comparing the velocities with that of Kearey *et al.* [3], and Azwin *et al.* [1], the first layer is the weathered layer and is likely to be dry sand. It has average thicknesses of 12.49 m, 9.17 m, 11.71 m, and 11.73 m respectively for the four profiles. The second layer is likely to be saturated sand which is the aquifer layer and has average thicknesses of 2.9 m, 2.8 m, 2.0 m and 2.3 m at depths of 12.49 m, 9.17 m, 11.71 m and 11.73 m respectively. The third layer which is likely to be sand stone (the confined aquifer) at depths 15.39 m, 11.97 m, 13.66 m, and 13.99 m, and has infinite thicknesses along the profiles.

4. Conclusion

It is concluded from the 2D seismic refraction results that the weathered layer thickness and aquifer depth varies from the Earth's surface in the four profiles. Though the weathered layer thicknesses and aquifer depths are relatively the same in average along the first, third and fourth profiles, the second profile is considered to reduce cost while sinking a borehole. The layers of the four profiles which are made up mainly sand and sand stones are the same because they have equivalent velocity range. The environments are good for structures, and multi storey buildings erect will not collapse provided the foundations are carried out properly.

References

[1] Azwin IN, Saad R, Nordiana M. Applying the seismic refraction tomography for site characterization. APCBEE Procedia, 2013; 5: 227-231.

[2] Igboekwe MU, Ohaegbuchu HE. Investigation into the weathering layer using up hole method of seismic refraction. J. Geol. Min. Res., 2011; 3: 73-86.

[3] Kearey P, Brooks M, Hill I. An introduction to geophysical exploration (3rd ed.). Blackwell Science Ltd. 2002.

[4] Cardarelli E, de Nardis R. Seismic refraction, isotropic and anisotropic seismic tomography on an ancient monument (Antoniuo and Faustina temple AD 141). Geophysical Prospecting, 2001; 49. 228 – 241.

[5] Obaje NG. Geology and Mineral Resources of Nigeria. Springer Dordrecht Heidelberg London New York. 2009.

[6] Reijers TJ. A Stratigraphy and sedimentology of the Niger Delta. Geologos, 2011; 17(3): 133–162.

[7] Ajaegwu NE, Odoh BI, Akpunonu EO, Obiadi II, Anakwuba EK. Late Miocene to Early Pliocene Palynostratigraphy and Palaeoenvironmentsof ANE-1 Well, Eastern Niger Delta, Nigeria. Journal of Mining and Geology, 2012; 48 (1): 31–43.

[8] Onema A, Lucas FA, Dada S. Palynocycles, palaeoecology and systems tracts concepts: A Case Study from the Miocene Okan-1 Well, Niger Delta Basin, Nigeria. Applied Ecology and Environmental Sciences, 2015; 3 (3): 66-74.

[9] Sandmeier KJ. Reflexw 3.0 manual, Sandmeier Software, Zipser Strabe 1, D-76227 Karlsruhe, Germany, 2002.

[10] Ray_tracing. In Wikipedia. Retrieved December, 2017, from https://en.m.wikipedia.org/wiki/Ray_tracing_(physics).

To whom correspondence should be addressed: Dr. Rasaq Bello, Department of Physics, Federal University Kashere, Gombe State, Nigeria